Appl Phys B (2009) 96: 111–117
DOI 10.1007/s00340-008-3349-z

Applied Physics B
Lasers and Optics

Frequency stabilization of CO laser using RF optogalvanic Lamb-dip

Y.-H. Lien · D.-K. Liu · J.-T. Shy

Received: 21 November 2008 / Revised version: 5 December 2008 / Published online: 30 December 2008

Abstract The Lamb dip of CO rovibrational transition is detected by a room temperature extracavity RF optogalvanic cell and employed to stabilize the frequency of a CO laser. The S/N ratio of optogalvanic signal is about 2000 $Hz^{-\frac{1}{2}}$ at optical power < 1 W. The relative depth of Lamb dip is 2.3%. The S/N ratios of first and third harmonic demodulated saturation signals are about 40 $Hz^{-\frac{1}{2}}$ and 10 $Hz^{-\frac{1}{2}}$, respectively. The CO laser is stabilized using the first harmonic demodulated signal, and the frequency stability is better than 300 kHz.

Concurrently, the influences of operational parameters, which include the coil current, partial pressures of gas mixture, are investigated. A simple model for the influence of coil current is presented, and further improvements are addressed as well.

PACS 42.55.Lt · 42.62.Fi

1 Introduction

High precision spectroscopy serves as an important approach to acquire detail information of molecules [1], and the related frequency standards and the frequency stabilization techniques are indispensable for these studies. The CO laser, which can lase on more than 150 lines with power up to several watts, is one of few readily available coherent sources in 5–7 μm, in which more than 80,000 molecular rovibrational lines are collected in HITRAN database [2]. However, the application of CO laser on spectroscopy is severely limited by its small spectral coverage (≈200 MHz around each line), and several spectroscopic techniques, such as Doppler-tuning [3, 4], laser magnetic resonance [5, 6], and microwave sideband generation [7–9], have been implemented to alleviate the limit. Moreover, the rovibrational transitions of CO are long regarded as the frequency standard candidates in this spectral region, and the related frequency stabilization techniques are worth studying.

The transitions of ordinary continuous wave CO laser are closely spaced, and two to three lines usually oscillate at the same grating position. The power profile is a jumbled composite of the power profiles of individual lines, irregularly offset from one and another. Therefore, appropriate schemes to reduce the interferences between these lines are necessary for laser frequency stabilization. De Serio et al. [10] uses a Fabry–Pérot interferometer as a tracking filter to eliminate the influence of other coexisting laser lines. They are able to stabilize a CO laser to the power profile extremes of the selected line. Although the stability they achieved is better than 100 kHz, the reproducibility is limited to several MHz since it is susceptible to the laser operating conditions.

The most successful scheme for CO laser frequency stabilization is the DC optogalvanic Lamb-dip stabilization, which is first achieved by Schneider et al. [11]. The optogalvanic effect is the change in the electric conductivity of a discharge caused by illuminating the discharge with the radiation which is resonant with an atomic or molecular transition in the discharge. In optogalvanic Lamb-dip stabilization, the Lamb dip is observed in a low pressure discharge optogalvanically and used to stabilize the laser frequency. Besides CO laser, the stabilization scheme has been applied to the regular and sequence bands CO_2 lasers [12, 13] successfully.

Y.-H. Lien (✉) · D.-K. Liu · J.-T. Shy
Department of Physics, National Tsing Hua University, Hsinchu, Taiwan 30013, ROC
e-mail: yhlien2004@gmail.com
Fax: +886-3-5723052

A sealed-off −80°C low pressure DC optogalvanic cell, which is filled with CO, Xe, and N_2, is placed inside CO laser cavity to detect the saturation signal. The third harmonic demodulated saturation signal is used to stabilize the laser frequency. The stability is reported to be better than 100 kHz. The frequency measurements of CO rovibrational transitions [14–16] are based on this scheme except the fundamental band of CO, which is done by conventional saturation spectroscopy [17].

The adoption of optogalvanic saturation spectroscopy is due to the very weak absorption of CO laser lines, which usually involve the transitions between high vibrational states in a DC discharge CO gas cell. The populations of these high vibrational states and their differences are small in such a cell. Our preliminary spectroscopic study of CO DC discharge shows that the absorption is too weak to be detected via absorption spectroscopy. Consequently, the highly sensitive optogalvanic spectroscopy is favored for the study.

Although DC optogalvanic Lamb dip [11] offers excellent performance, it is less favorable for daily operation due to low temperature cooling, carbon deposition on the cathode, and high cost of Xe. Therefore, the RF optogalvanic Lamb-dip stabilization is sought as an alternative. The RF optogalvanic Lamb dip has been successfully applied to CO_2 laser frequency stabilization [18, 19].

In this paper, we report our study on the optogalvanic effect of CO:Ar mixture, and the frequency stabilization of CO laser using RF optogalvanic Lamb-dip. The first harmonic demodulated saturation signal is exploited for frequency stabilization. The RF optogalvanic system continuously operates for several weeks without any maintenance. The frequency stability, which is mainly limited by the S/N ratio, is better than 300 kHz, and does not outpace the DC scheme.

2 Experimental setup

The experimental setup is shown in Fig. 1. The sealed-off CO laser is built on the design of Freed [20]. The cavity is formed by a 150 lines/mm Littrow-mounted grating and a concave Ge output coupler ($R = 3$ m) which is mounted on a PZT. The total length is about 1.51 m, and the corresponding mode spacing is about 99 MHz. The laser discharge tube is enclosed by a cooling jacket and a vacuum jacket for thermal insulation. The discharge tube is filled with 18 torr of CO, N_2, Xe, and He mixture with the ratio 6.25% : 6.25% : 6.25% : 81.25%. The cooling jacket is maintained at −60°C by an ethanol-circulated refrigerator. The maximum output power is about 1 W. There are about 150 laser lines available in 5–7 μm. Two lines simultaneously lase at most grating positions. In order to reach the desired saturation intensity, a pair of concave and convex mirrors ($R = \pm 1$ m), are used to focus the laser beam into the RF optogalvanic cell. The incident laser beam is reflected and focused with a small angular deviation by a concave mirror $R = 7.5$ m. The gas cell is placed 5 m away from the laser for good beam overlapping within it and suppressing optical feedback. An optical chopper is inserted when the characteristic study of optogalvanic signal is performed. The optogalvanic signal is obtained by a lock-in amplifier and the time constant is set to 300 ms in all experiments.

As the amplitude variation is detected as the signal, it is indispensable to construct an amplitude stable RF oscillator for optogalvanic spectroscopy. The oscillator developed by May [21] is used because its self-limiting characteristic and simple construction. The oscillator comprises of a common-emitter RF amplifier, a feedback LC network, and an envelope detector. The schematic diagram is shown in Fig. 2. It is almost identical to the original design except some modifications on the envelope detector. The frequency of this oscillator is between 12 and 14 MHz. The coil L1, L2, and L3 represent individual segment of the discharge coil. This central tap of the coil is grounded. The collector of the amplifier is connected to one turn from the central tap. This design can prevent the amplification stage from damaging by the ignition spark, which is caused by the Tesla coil. It also allows us to use low voltage RF transistors which are cheaper and easier to find. The turns of the coil are raised to 50 to keep the discharge stable at higher pressure. The length and diameter of this coil are about 100 mm and 16 mm, respectively. The inductance of this coil is estimated as 460 μH. An air gap variable capacitor is used for the capacitor VC1 because the usual capacitor trimmer is not appropriate to maintain low-noise discharge. A shunt resistor 24.9 kΩ, which connects the output of AC-coupled capacitor C1 to ground, is introduced to reduces the noise of the envelope detector output. The coil current is set by the potentiometer VR1, and the discharge is stabilized by tweaking the variable capacitor VC1. The amplitude noise is as small as 10 nV $\mathrm{Hz}^{-\frac{1}{2}}$ between 180 and 500 Hz. Moreover, it is insensitive to the environment disturbance and no metal cage is needed to shield the system.

The gas cell is made by a 30 cm long, inner diameter 12 mm Pyrex tube with CaF_2 Brewster windows on both ends and is pumped by an 100 l/min mechanical pump. The ultimate pressure is 10 mtorr. The partial pressures of gas mixture are regulated by the corresponding needle valves.

3 Results

The optogalvanic spectrum and the corresponding laser power profile are acquired by scanning the laser cavity length and chopping the laser beam simultaneously, and one set of typical results are shown in Fig. 3. These profiles are the composites of the contributions from the coexisting lines

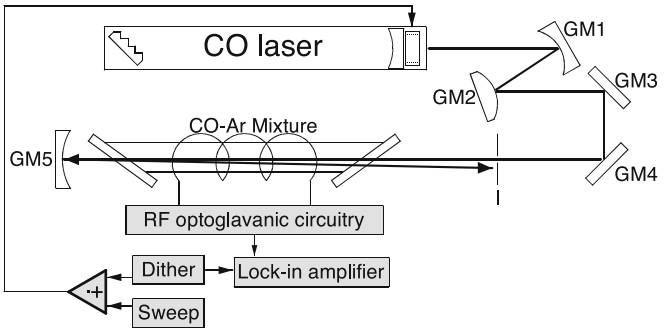

Fig. 1 The apparatus of CO RF optogalvanic system. GMx: Gold-coated mirrors. I: Iris

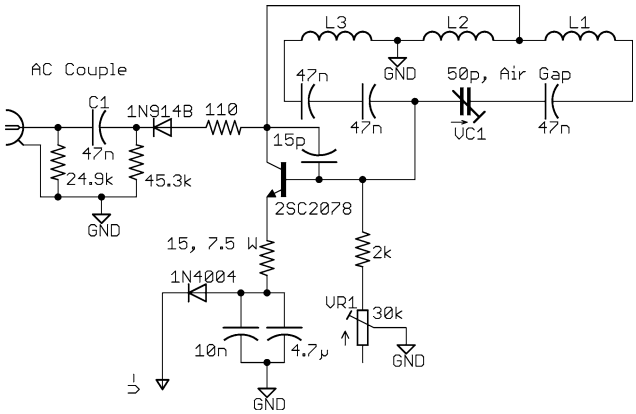

Fig. 2 The inductive-coupled RF oscillator

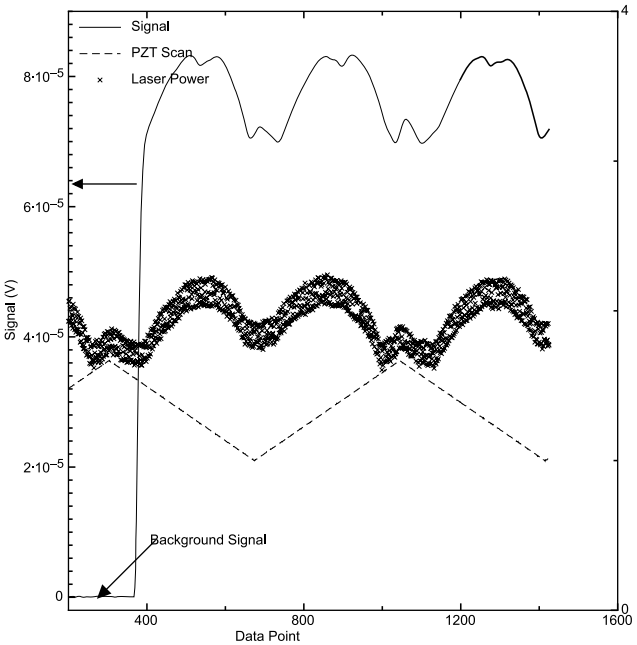

Fig. 3 The RF optogalvanic signal of CO rovibrational transitions. The laser beam is blocked at the beginning to show the background of RF optogalvanic signal. Here the optimal conditions (see text) are used

because of above mentioned multi-line characteristic of CO laser. As long as the frequency difference of the coexisting laser lines is not a multiple of the laser mode spacing, the peaks of individual line will not be coincident. As shown in the Fig. 3, the peak separation between coexisting laser lines can be identified by the asymmetry of power profile. The close separation of the coexisting lines may cause serious problems on seeking the saturation dip of one line since it is distorted by the optogalvanic signal from another line. To confirm the saturation dip, several measures such as blocking the retroreflected beam, checking the separation of coexisting lines by a home-made Fabry–Pérot interferometer, are taken.

The simultaneous lasing of 14P(12) and 15P(5) lines are identified in Fig. 3 by the homemade Fabry–Pérot interferometer, and their power ratio is about 5:2 when the line 14P(12) is tuned to its peak. The coincidence between the saturation dip and the power peak of 14P(12) is verified as well. The dip width is estimated to be about 7.3 MHz. The influence of the weak line can be recognized by a small bulge on one side of the dip.

We also find few extraordinary optogalvanic responses at some specific CO laser lines. These extraordinary lines exhibit 2–3 times larger responses than other lines. By lowering the partial pressure of CO until the optogalvanic signal of ordinary lines vanish completely, these extraordinary lines are still strong. In addition, no saturation dips are observed on these lines. We suspect that it is due to other atomic/molecular species in the discharge. The transitions of Ar I [22] are compared, but none are close to the available CO laser lines. The origins of these lines are still unknown yet.

The influence of the gas mixture is investigated extensively to determine the optimums for frequency stabilization. The addition of N_2 is conventionally considered to be important for transferring excitation energy to CO. However, our study shows that the addition of N_2 severely diminishes signal strength and introduces some extent of discharge instability. Although preliminary study indicates that CO–Xe mixture produces higher optogalvanic signal than CO–Ar mixture, we focus our study on CO–Ar mixture due to practical reason.

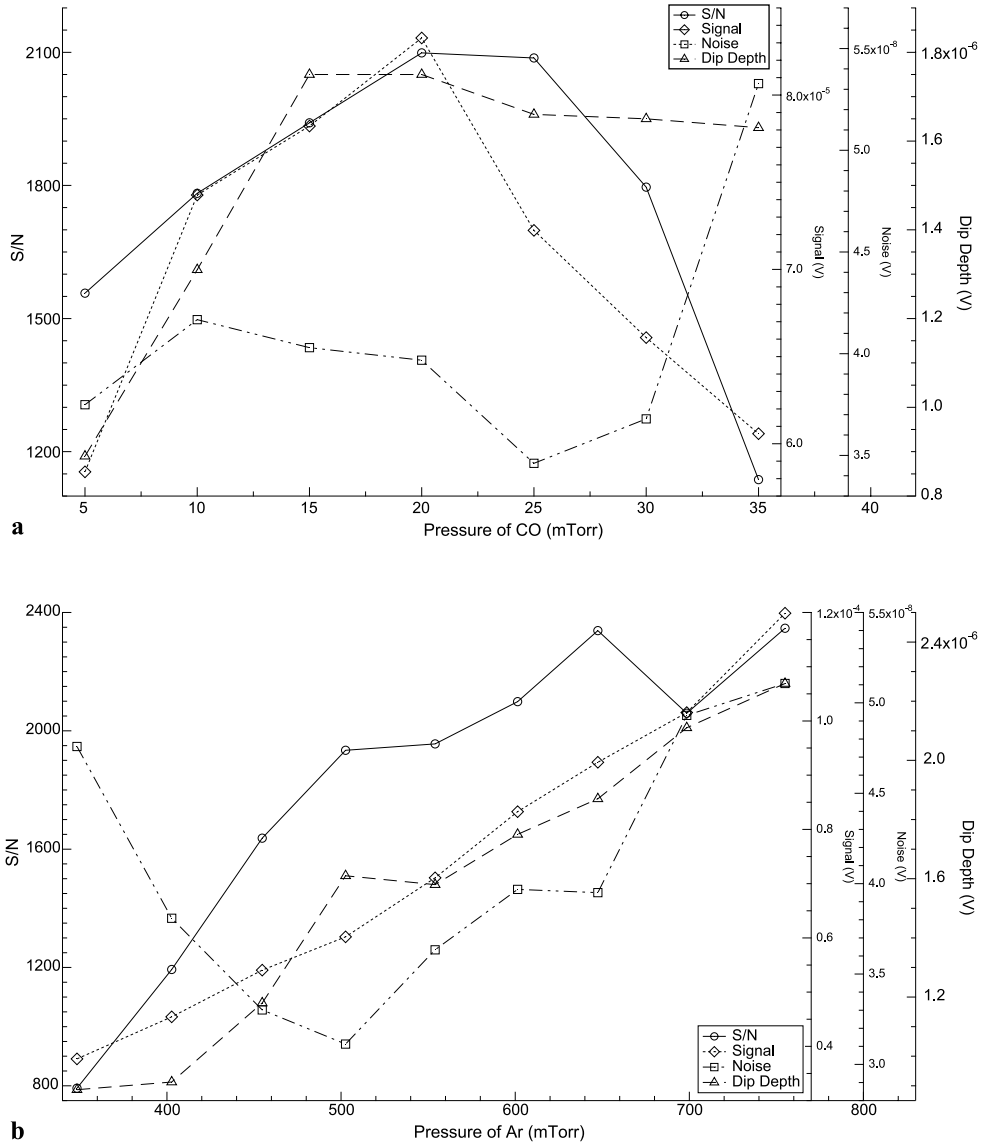

Fig. 4 The optogalvanic signal versus gas partial pressure. (**a**) Partial pressure of CO. (**b**) Partial pressure of Ar

The optimal gas mixture is determined by the S/N ratio divided by the width of saturation signal. The frequency discrimination is proportional to this ratio. Our study shows the optimums of the partial pressures of CO and Ar are 20 mtorr and 600 mtorr. Figure 4(a) shows the dependence of optogalvanic signal on CO pressure with 600 mtorr Ar pressure. The signal is very sensitive to the CO pressure. Surprisingly, the optimal concentration of CO is very low in comparison with the DC optogalvanic signal [11]. In fact, high concentration of CO completely ruins the optogalvanic signal and also causes the discharge unstable. Figure 4(b) shows the dependence of the optogalvanic signal on Ar pressure with 20 mtorr CO pressure. The signal strength increases as the partial pressure of Ar increases in the experimental range.

The dependence of the optogalvanic signal on modulation frequency is shown in Fig. 5. The drop of signal at low frequency is due to the AC couple envelop detector of the RF oscillator and the decrease at high frequency is caused by the molecular relaxation. There is a noise peak at 270 Hz. To avoid this peak, the modulation frequency is set at 255 Hz for the rest of the experiments.

Figure 6 shows the optogalvanic signal increases monotonically with the coil current of the RF oscillator. It can be easily explained by the mechanism of optogalvanic effect. The gas cell is placed within the coil and the gas mixture is excited by RF field. The electrical impedance of discharge is determined by [23]

$$Z = \frac{m}{e^2}\frac{\nu_e}{n_e}l,$$

$$\nu_e \propto n_e \sigma_e,$$

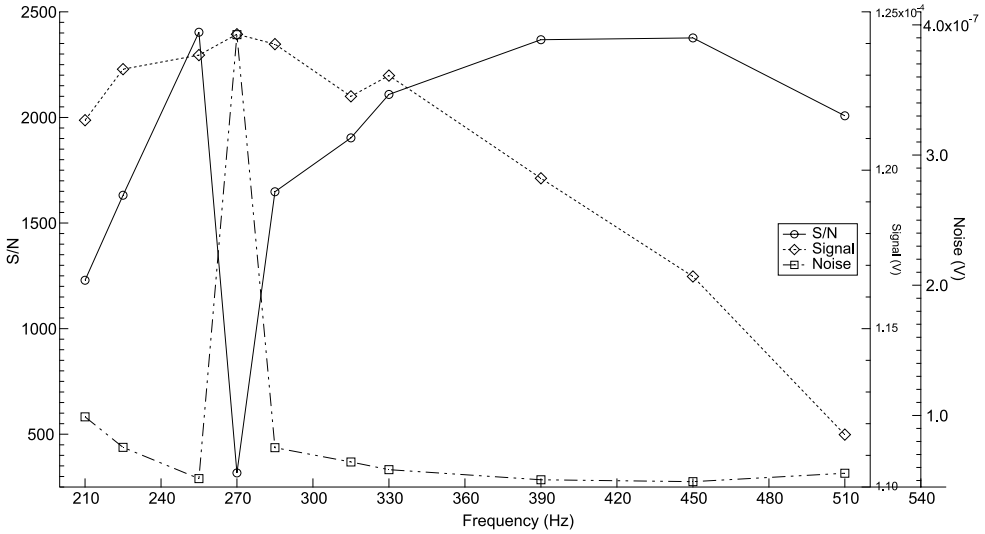

Fig. 5 The RF optogalvanic signal verse chopping frequency

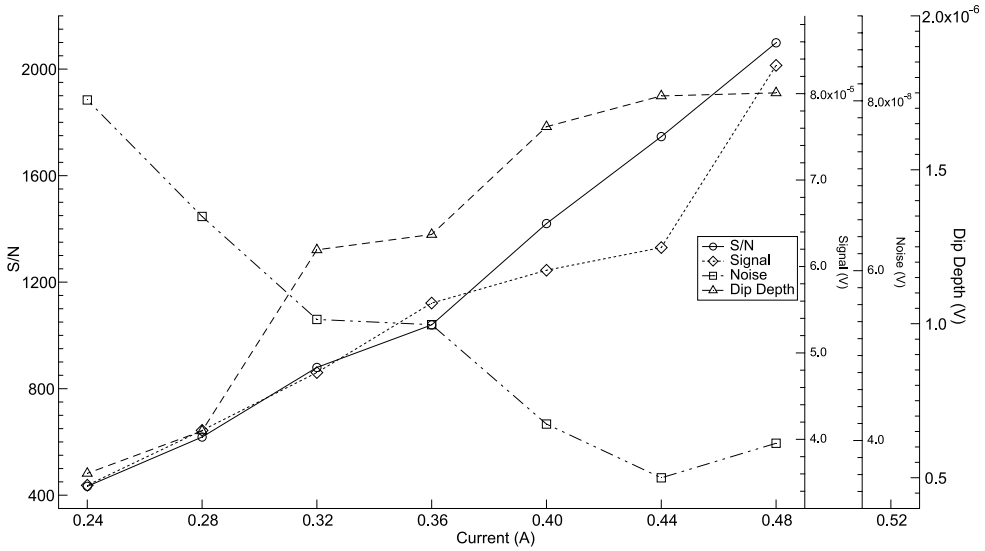

Fig. 6 The optogalvanic signal versus coil current. These data are acquired with optimal condition except coil current

and

$$Z \propto \sigma_e l,$$

where m, ν_e, n_e, σ_e, and l represent electron mass, electron density, collision frequency of electrons, the effective electron–molecule collision cross-section, and the length of discharge region, respectively. Concerning the internal structures of molecules, the cross-section σ_e is supposed to be contributed by the electron–molecule collision cross sections σ_i for ith molecular state and the corresponding population n_i:

$$\sigma_e = \sum_i \sigma_i n_{i.}$$

As the frequency of incident light is resonant with a molecular transition, the internal population distribution changes and the effective collision cross-section changes correspondingly. That means the electrical impedance of the discharge tube will change as the absorption occurs:

$$\delta Z \propto \delta\sigma_e = \sum_i \sigma_i \delta n_i.$$

Assuming the small impedance change, the oscillation frequency and the saturated current gain of amplifier will remain constant. Therefore, the current flowing through the coil does not change whether the incident light is resonant or not. However, the change of impedance will induce RF amplitude variation across the coil

$$V_{\mathrm{OG}} \equiv \delta V \propto I \sum_i \sigma_i \delta n_i, \tag{1}$$

where I is the coil current. The population variation is known as

$$\delta n_i \propto F\sigma_{\text{abs}} n_i \propto F\sigma_{\text{abs}}\sigma_{\text{ex}}^{i} n_e, \tag{2}$$

where F, σ_{abs}, σ_{ex}^{i}, and n_e represent optical intensity, the cross-section for optical absorption, electronic excitation from ground state and electron density within the discharge tube, respectively. Moreover,

$$n_e \propto I. \tag{3}$$

Combining (1), (2), and (3),

$$\delta n_i \propto I.$$

Therefore, the relation between optogalvanic signal and coil current will be given in quadric form

$$V_{\text{OG}} \propto I^2. \tag{4}$$

This amplitude variation V_{OG} is then detected as the optogalvanic signal by rectifying the RF signal with an envelope detector. It clearly shows the optogalvanic signal will benefit from the higher coil current. Figure 7 shows the fitting curve of the equation $V_{\text{OG}} = aI^2 + b$. The constant b is introduced as the offset, which may be brought by the instruments. The fitting is quite close to the experimental curve and the proposed model seems to give a good account for the relations between the optogalvanic signal and the coil current.

Combining above experimental results, we can determine the optimal conditions for CO optogalvanic Lamb-dip stabilization, namely the partial pressure of CO and Ar is 20 mtorr and 600 mtorr, the modulation frequency is 255 Hz, and the coil current is 0.48 A. As shown in Fig. 3, the S/N ratio of composite signal is about 2200 $\text{Hz}^{-\frac{1}{2}}$. The S/N ratio of the dip is about 50 $\text{Hz}^{-\frac{1}{2}}$. Assuming the optogalvanic responses of two lines shown in Fig. 3 are same, the S/N of 14P(12) is expected to be more than 1500 $\text{Hz}^{-\frac{1}{2}}$.

To stabilize the laser frequency, the first harmonic demodulated spectrum is obtained by modulating the laser frequency through the laser PZT and it is used as the error signal. A typical first harmonic demodulated signal is shown in Fig. 8. The S/N ratio of saturation dip is about 40 $\text{Hz}^{-\frac{1}{2}}$. The frequency stabilization had been tried and the result is shown in Fig. 9. The relative stability is better than 300 kHz, according to the fluctuation of the error signal.

We also try the third harmonic demodulated spectroscopy, and the data are shown in Fig. 10. The optimum modulation depth is about 11.5 MHz. The S/N ratio is estimated to be about 10 $\text{Hz}^{-\frac{1}{2}}$.

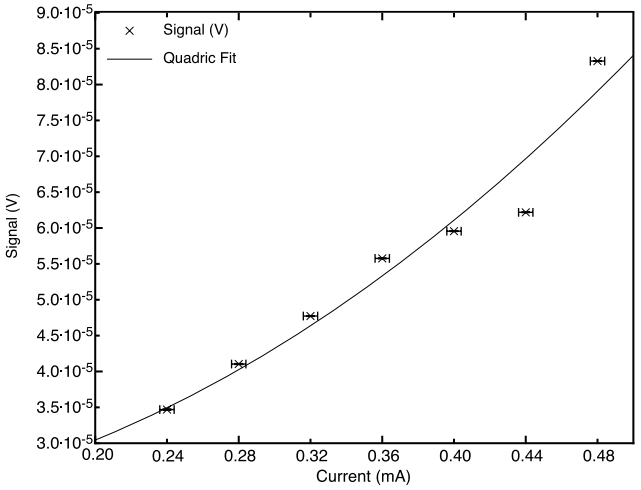

Fig. 7 The quadric fitting for signal verse coil current. The error of the signals are too small to see because of a high S/N ratio

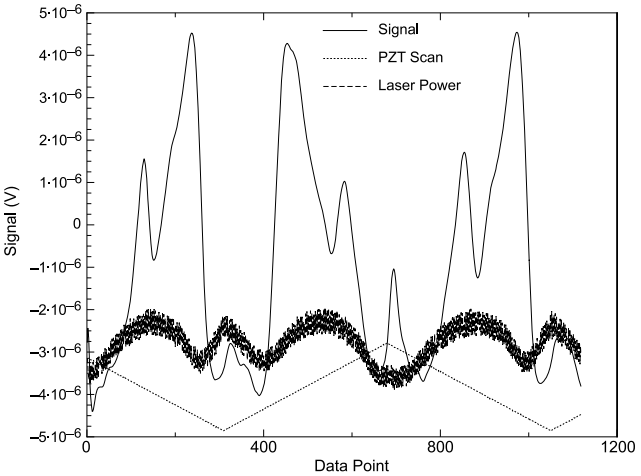

Fig. 8 The optimal first harmonic demodulated optogalvanic signal

4 Conclusions

The characteristics of low pressure CO–Ar RF optogalvanic spectroscopy are investigated. The saturation dip observed optogalvanically is used to stabilize the CO laser frequency and the frequency stability is about 300 kHz. The RF optogalvanic Lamb-dip is very simple, robust, and cheap in comparison with the DC optogalvanic Lamb-dip. This system is capable to operate continuously for weeks without any maintenance. The S/N ratio of third harmonic demodulated saturation signal is believed to be comparable with the DC optogalvanic Lamb-dip if the RF discharge cell is placed inside the laser cavity. Some simple improvements are expected, e.g., replacing the Ar by Xe or increasing the coil current and the coil turns of the RF oscillator.

The performance of this system is mainly limited by the problems caused by the undesired laser line. These problems include the broadening, asymmetry of the saturation

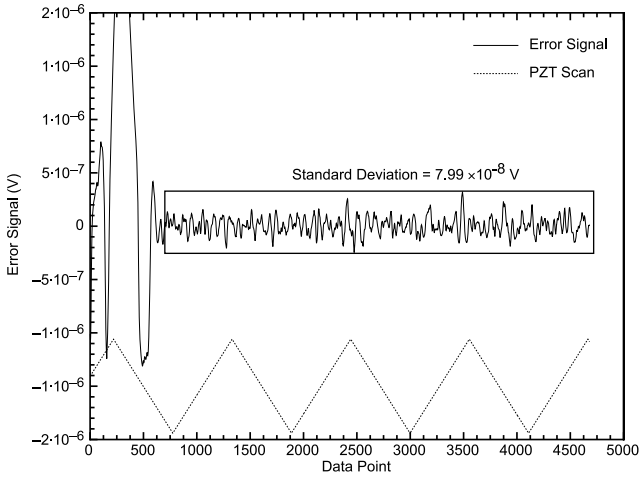

Fig. 9 The result of frequency stabilization. The right portion of the trace is the error signal. The magnitude of error signal is 7.99×10^{-8} V

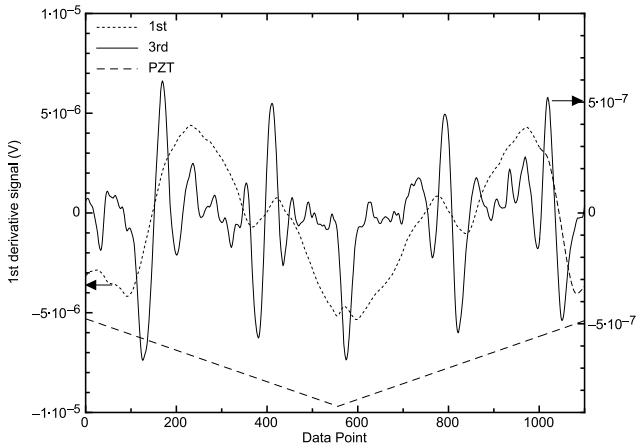

Fig. 10 The first and third harmonic demodulated optogalvanic signal

dip, and a redundant background for wavelength modulation spectroscopy which cause an offset in frequency locking. The cavity-enhanced RF optogalvanic spectroscopy by placing the RF discharge cell inside an optical resonator is believed to be the best solution because of complete filtering out the undesired laser line and the same advantages enjoyed by intracavity DC optogalvanic scheme, e.g., perfect beam overlapping and high intracavity intensity.

Finally, the origin of extraordinary optogalvanic response, the absence of N_2 and the unexpected low CO concentration for optimal signal strength are still unknown. To answer these questions, more experimental investigations and theoretical modeling need to be performed.

Acknowledgements We would like to express our great gratitude to Prof. W.H. Wing, University of Arizona for loaning the CO laser system. We also thank Dr. Chen-Ning Chu for discussions on the RF discharge circuit. This work is supported by the National Science Council of Taiwan, ROC under grant number NSC95-2112-M-007-002.

References

1. M. Herman, J. Lievin, J. Auwera, A. Campargue, in *Global and Accurate Vibration Hamiltonians from High-Resolution Molecular Spectroscopy* (Wiley-Interscience, New York, 1999), p. 95
2. http://www.cfa.harvard.edu/HITRAN/
3. W.H. Wing, G.A. Ruff, W.E. Lamb, J.J. Spezeski, Phys. Rev. Lett. **36**, 1488 (1976)
4. J.-T. Shy, J.W. Farley, W.E. Lamb, W.H. Wing, Phys. Rev. Lett. **45**, 535 (1980)
5. W. Rohrbeck, A. Hinz, P. Nelle, M.A. Gondal, W. Urban, Appl. Phys. B: Photo. Phys. **31**, 139 (1983)
6. Z.-A. Liu, Y.-Y. Liu, F.-Y. Li, J.-R. Li, K.-L. He, B.-Z. Gong, Y.-Q. Cehn, Chem. Phys. Lett. **183**, 340 (1991)
7. S.-C. Hsu, R.H. Schwendeman, G. Magerl, IEEE J. Quantum Electron. **24**, 2294 (1988)
8. B. Meyer, S. Saupe, M.H. Wappelhorst, T. George, F. Kuhnemann, M. Schneider, M. Havenith, W. Urban, J. Legrand, Appl. Phys. B: Lasers Opt. **61**, 169 (1995)
9. U. Merker, P. Engels, F. Madeja, M. Havenith, W. Urban, Rev. Sci. Instrum. **70**, 1933 (1999)
10. R. De Serio, G.A. Ruff, W.H. Wing, IEEE J. Quantum Electron. **20**, 140 (1984)
11. M. Schneider, A. Hinz, A. Groh, K.M. Evenson, W. Urban, Appl. Phys. B: Photophys. Laser Chem. **44**, 241 (1987)
12. J.T. Shy, T.C. Yen, Opt. Commun. **60**, 306 (1986)
13. J.T. Shy, T.C. Yen, Opt. Lett. **12**, 325 (1987)
14. M. Schneider, K.M. Evenson, M.D. Vanek, D.A. Jennings, J.S. Wells, A. Stahn, W. Urban, J. Mol. Spectrosc. **135**, 197 (1989)
15. M. Schneider, J.S. Wells, A.G. Maki, J. Mol. Spectrosc. **139**, 432 (1990)
16. A.G. Maki, J.S. Wells, D.A. Jennings, J. Mol. Spectrosc. **144**, 224 (1990)
17. T. George, B. Wu, A. Dax, M. Schneider, W. Urban, Appl. Phys. B: Photophys. Laser Chem. **53**, 330 (1991)
18. C.-Y. Shieh, C.-C. Chou, C.-C. Chen, T.-M. Huang, J.-D. Chern, T.-C. Yen, J.-T. Shy, Opt. Commun. **88**, 47 (1992)
19. C.-C. Tsai, T. Lin, C.-Y. Shieh, T.-C. Yen, J.-T. Shy, Appl. Opt. **30**, 3842 (1991)
20. C. Freed, Appl. Phys. Lett. **18**, 458 (1971)
21. R.D. May, P.H. May, Rev. Sci. Instrum. **57**, 2242 (1986)
22. W. Whaling, W.H.C. Anderson, M.T. Carle, J.W. Brault, H.A. Zurem, J. Res. Natl. Inst. Stand. Technol. **107**, 149 (2002)
23. Y. Raizer, *Gas Discharge Physics* (Springer, New York, 1997)